sciendo

POLISH MARITIME RESEARCH 4 (104) 2019 Vol. 26; pp. 149-156
10.2478/pomr-2019-0077

INVESTIGATION OF THE COMBUSTION PROCESSES IN THE GAS TURBINE MODULE OF AN FPSO OPERATING ON ASSOCIATED GAS CONVERSION PRODUCTS

Oleksandr Cherednichenko
Admiral Makarov National University of Shipbuilding, Ukraine
Serhiy Serbin
Admiral Makarov National University of Shipbuilding, Ukraine
Marek Dzida
Gdańsk University of Technology, Poland

ABSTRACT

In this paper, we consider the issue of thermo-chemical heat recovery of waste heat from gas turbine engines for the steam conversion of associated gas for offshore vessels. Current trends in the development of offshore infrastructure are identified, and the composition of power plants for mobile offshore drilling units and FPSO vessels is analyzed. We present the results of a comparison of power-to-volume ratio, power-to-weight ratio and efficiency for diesel and gas turbine power modules of various capacities. Mathematical modeling methods are used to analyze the parameters of an alternative gas turbine unit based on steam conversion of the associated gas, and the estimated efficiency of the energy module is shown to be 50%. In the modeling of the burning processes, the UGT 25000 serial low emission combustor is considered, and a detailed analysis of the processes in the combustor is presented, based on the application of a 35-reaction chemical mechanism. We confirm the possibility of efficient combustion of associated gas steam conversion products with different compositions, and establish that stable operation of the gas turbine combustor is possible when using fuels with low calorific values in the range 7–8 MJ/kg. It is found that the emissions of NOx and CO during operation of a gas turbine engine on the associated gas conversion products are within acceptable limits.

Keywords: thermo-chemical heat recovery,gas turbine engine,associated gas,combustor

INTRODUCTION

Oil and gas production on the sea and ocean shelf is currently one of the main sources of global energy resources, and has a significant impact on the economies of both individual countries and entire regions. Shallow-water production has been exploited for a long time, and now accounts for over 30% of global oil production and 25% of gas production. There are significant oil and gas deposits in the deep-sea areas of the world's oceans, but their development requires large financial investments and the introduction of new technologies.

A large and diverse fleet of offshore vessels [1] has been created to support work on offshore fields (Fig. 1).

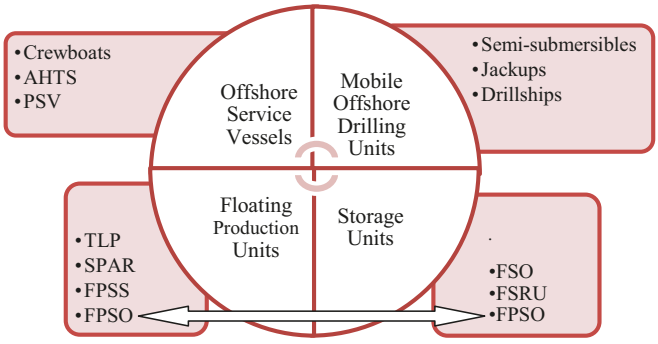

Fig. 1. Offshore vessels and floating units. Abbreviations: AHTS – Anchor Handling Tug Supply Vessel; PSV – Platform Supply Vessel; TLP – Tension-Leg Platform; SPAR – Spar Platform; FPSS – Semisubmersible Floating Production System; FPSO – Floating Production Storage And Offloading System; FSO – Floating Storage Offloading Unit; FSRU – Floating Storage And Regasification Unit

Floating offshore infrastructure includes major ship groups and floating units such as offshore service vessels (OSVs), mobile offshore drilling units (MODUs), floating production units and storage units.

IDENTIFICATION OF THE INVESTIGATION OBJECT

One of the main factors ensuring the efficient operation of the first link in the supply chain (i.e. production, transportation and supply) of offshore oil and gas is related to the energy efficiency indicators of offshore vessels and floating units. MODU and floating production storage and offloading (FPSO) installations are of primary interest in energy efficiency research. The production systems on such vessels determine the stability and efficiency of production processes, and those of FPSOs determine the processing and shipping efficiency. These processes involve significant energy consumption. The composition and characteristics of the installations of the offshore infrastructure object vary widely, but The main drive engines are typically gas turbine engines (GTEs) and medium speed four-stroke diesel engines (4SDEs).

Deep-water platforms and drilling vessels can operate at depths of over 3.5 km. Extraction at great depths is expensive: the cost of newly built drilling vessels can reach 900 million USD, and for semi-submersible platforms, this may be 600 million USD. All semi-submersible platforms and drillships incur additional energy costs, since they are equipped with powerful dynamic positioning systems, and fuel costs can reach 100,000 USD per day [2]. For drilling ships and platforms, 4SDEs are preferred. For example, the installation on the drilling ship Stena Drill MAX consists of six main engines to drive the vessel's main generators, and each Wärtsilä 16V32 engine has an output of 7.3 MW [3]. The Stena Don semi-submersible floating drill platform consists of nine Wartsila 16V25 main generators (3.5 MW each) [4]. The Aker H-6e semi-submersible floating drill platform consists of eight main Rolls Royce diesel engines (5.3 MW each) [5].

It should be noted that despite the high capital (CAPEX) and operating (OPEX) expenses, the share of deep-sea production is increasing, and has a significant impact on the global economy. This is evidenced by the fact that analytical reviews and forecasts of regional hydrocarbon energy markets are based on an assessment of the key factors of onshore and offshore oil and gas production, taking into account an analysis of the situation with respect to shallow and deepwater production [1].

The increase in production in deep-sea regions and areas remote from ground infrastructure has also led to an increase in the number of FPSO vessels. At the end of 2018, 183 FPSO vessels were operating in the offshore fleet, and according to forecasts, another 55 such vessels will be built by 2022 [6, 7]. FPSO power plants are characterized by the presence of gas turbine and combined type installations. Thus, on the FPSO vessel Global Producer III, the power plant consists of two 16 MW Alstom GT 35 gas turbines and waste heat recovery units that provide all of the heat for the oil separation process [8]. The general power plant of the Armada Olombendo FPSO consists of three 21 MW dual fuel turbines [9]. This FPSO's Dhirubhai-1 power plant contains of three 4 MW gas turbine generators and two main boilers, giving a total capacity of 88 t/h for three 5 MW and two 1 MW steam turbine generators [10]. The FPSO's Pioneiro de Libra installation provides three 27.5 MW gas turbine generators, which operate at 50% load, and four diesel generators [11]. The FPSO's Cidade de Itajaí installation consists of four gas turbine generators with 36 MW of power, and two 2 MW diesel generators [12]. Power generation on the FPSO TRITON is provided by two LM6000 gas turbines (42 MW ISO rating) [13].

Leading manufacturers of power equipment have developed power modules for MODUs and FPSOs with diesel generators (DGs) and gas turbine generators (GTGs) [1416].

The following indicators can be used as criteria for comparing the characteristics of energy modules:

$\dot{V} = P_e/V_m$, power-to-volume ratio, where P_e is the power generated by the module (kW) and V_m the module volume (m^3).

$\dot{M} = P_e/M_m$, power-to-mass ratio, where M_m is the module weight (tons).

$\eta = P_e/(m_f \cdot LCV)$, module efficiency, where m_f is the fuel mass flux (kg/s) and LCV the low calorific value of the fuel (kJ/kg).

Figure 2 presents the results of a comparison of power-to-volume ratio, power-to-weight ratio and efficiency for diesel and gas turbine power modules of various capacities.

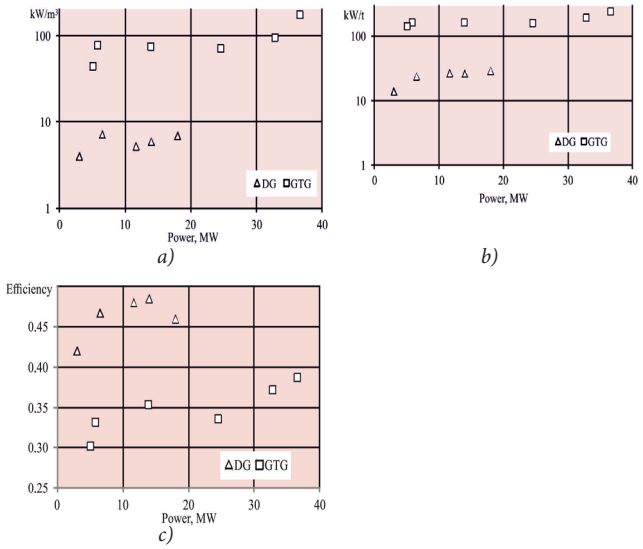

Fig. 2 Comparison of energy module characteristics for offshore vessels: (a) power-to-volume ratio; (b) power-to-mass ratio; (c) efficiency.

Abbreviations: DG 18V51/60DF (18 MW), 16CM46DF (14 MW), 12CM43C (11.6 MW), 12CM32C (6.5 MW), 6CM34DF (3 MW); GTG - SGT A35 (36.6 MW), SGT 700 (32.8 MW), SGT 600 (24.5 MW), SGT 400 (13.9 MW), SGT A05 (5.8 MW), SGT 100 (5 MW)

Energy modules based on gas turbine technologies have a significant advantage in terms of their mass and size characteristics, but are inferior to diesel options in terms of fuel efficiency. A number of publications have been devoted to improving the efficiency of marine power modules using

advanced and combined cycle plants [17, 18]. However, experience with offshore drilling platforms in Norway has shown that their large dimensions make combined cycle installations impractical for offshore vessels [19].

For FPSOs and MODUs, which operate in deep-sea and remote areas of production, the requirements for the mass and size of the equipment are the most stringent, as these are related to ensuring dependability. As shown in [20, 21], one effective means of ensuring the reliability of a ship's power plant is redundancy. Ship power plants, including offshore vessels, are characterized by the use of structural redundancy, which provides the ability to connect reserve power in case of failure of the main equipment. This practice is widespread in the offshore fleet; the use of a single unit to ensure basic production needs is considered undesirable, and in practice this does not apply. In [22], aspects of the running of 192 gas turbines operating in offshore infrastructure were considered, and based on the analysis presented in this study, it follows that the average load of gas turbine engines during operation is about 50%. A total of 97% of gas turbine engines operate as part of an energy module with more than one unit and with load sharing.

To reduce NO_x and CO emissions from offshore vessels, gas turbine engines with modified combustion systems known as dry low emissions (DLE) are used. Although in some cases the operation of gas turbine engines with DLE in partial load modes may increase the NO_x and CO emissions, and the fuel gas composition significantly affects performance [22], the use of such technology is promising. This article discusses the possibility of its applicability to an FPSO vessel equipped with a gas turbine module.

Thermo-chemical technologies are a promising direction for increasing the efficiency of heat engines, and can allow for the conversion of base fuel using the thermal energy of the exhaust gases. When such technologies are applied on offshore vessels, natural gas, associated petroleum gas of various compositions or gaseous fuel based on heavy hydrocarbons (ethane, propane, butane and others) can be used as the main fuel. Earlier studies [2326] have considered the use of thermo-chemical heat recovery from GTE exhaust gases for the steam conversion of LNG, methanol and associated gases of different compositions. Further analysis of the appropriateness and applicability of thermo-chemical technologies in the energy complexes of offshore vessels and floating drilling platforms requires investigation of the working processes in a gas turbine combustor operating on associated gas conversion products.

CHARACTERISTICS OF THE PROCESSES IN A GAS TURBINE COMBUSTOR OPERATING ON ASSOCIATED GAS CONVERSION PRODUCTS

Investigations carried out earlier by the current authors have made it possible to identify the main parameters that influence the process of associated gas conversion [26]. It was found that an increase in the process pressure leads to an increase in the temperature, which is necessary for effective conversion. In addition, a rise in pressure leads to an increase in the proportion of the steam that must be fed into the reactor. It is not possible to avoid conversion at a pressure of below 2–2.5 MPa, since the effective organization of the working processes in the gas turbine combustor requires that the fuel supply pressure exceed the air pressure behind the compressor.

Mathematical modeling methods [27] were used to analyze the parameters of an alternative gas turbine installation with steam conversion of associated gas (Fig. 3).

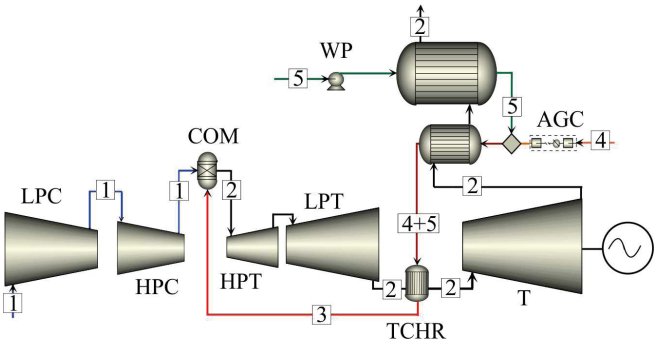

Fig. 3 Simplified calculation scheme for a power plant: 1 – air; 2 – gas; 3 – syngas; 4 – associated gas; 5 – water (steam); LPC – LP compressor; HPC – HP compressor; CAG – associated gas compressor; COM – combustor; SG – steam generator; LPT – LP turbine; HPT – HP turbine; T – power turbine; TCHR – thermo-chemical reactor; WP – water pump

The basic parameters of the UGT 25000 gas turbine simple cycle installation are adopted. This dual-rotor turbine engine with a free power turbine is designed for electric power generation, natural gas transportation and marine propulsion.

The investigations conducted here allowed us to determine the following:

- for a dual-rotor gas turbine engine, it is advisable to install a thermo-chemical reactor behind a low-pressure turbine;
- a significant increase in the volume of working fluid supplied to the reactor (and then to the combustor and the turbine flow section) requires the operation of serial gas turbine engines in partial mode when using the products of steam conversion of associated gas as the main fuel.

The following limitations of the turbocompressor unit were modeled:

- operation of the GTE at partial load mode;
- a fixed turbine inlet temperature;
- environmental parameters taken from ISO 19859: 2016.

Associated gas was adopted as the initial fuel, with the following composition (vol.): methane (CH_4) 62.8–73.7%; ethane (C_3H_8) 6.7–17.7%; propane (C_2H_6) 6.1–9.0%; butane (C_4H_{10}) 2.4–5.0%; pentane and heavier (C5+) 1.0–3.7%; carbon dioxide (CO_2) 0.6–9.2%; nitrogen (N_2) 0.0–4.4%; hydrogen sulfide (H_2S) 0.0–2.8 [26,28]. Since the gas temperature behind the steam generator was above the dew point temperature, the maximum allowable steam/gas mass ratio was 6–7, depending on the composition of the associated gas. The use

of thermo-chemical regeneration can increase the efficiency of the FPSO's gas turbine energy module by up to 50%.

By modeling the processes in the thermo-chemical heat recovery circuit, we established that the content of the initial associated gas slightly affects the composition of the synthesis gas. The main components of the synthesis gas obtained by thermo-chemical regeneration are hydrogen and steam. In this case, the low calorific values of the synthesis gas lie in the range 7–8 MJ/kg.

The UGT 25000 serial low emission combustor was used to model the burning processes. The combustor of a 25 MW power gas turbine engine has a cannular design (Fig. 4) in which dry combustion of a lean partially premixed mixture is carried out [29, 30]. The main element of this chamber is a burner consisting of two radial swirlers, one for each of the two channels, behind which the annular mixing chambers are located. The air flow distribution between the first and second swirlers as a percentage of total air flow through the flame tube is about 12–61 %. Gaseous fuel is supplied through a set of holes in the vanes of the radial swirlers in both channels.

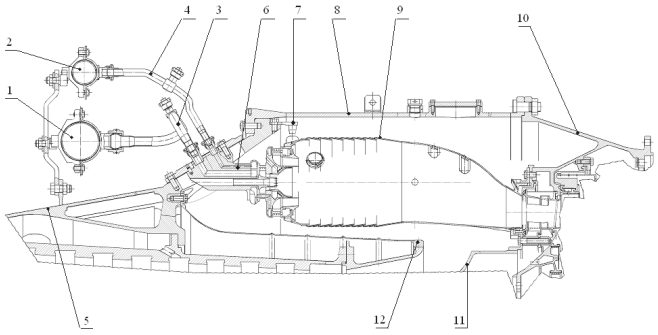

Fig. 4 Low-emission combustor of a GTE with power 25 MW: 1, 2 – collectors of the first and second channels; 3, 4 – delivery pipes of the first and second channels; 5 – compressor body; 6 – burner; 7 – holder; 8 – combustor casing; 9 – flame tube; 10 – load-carrying body; 11 – diffuser; 12 – inner casing

The modeling of physical and chemical processes in a gas turbine combustor is based on solutions to the differential equations of mass, impulse and energy conservation for the multi-component, turbulent, chemically reacting system [3135]. The equations for the conservation of mass can be written as follows:

$$\frac{\partial \rho}{\partial t} + \nabla \cdot (\rho \vec{v}) = S_m \tag{1}$$

where ρ is the fluid density, $\vec{v}$ is the velocity vector, and S_m is the mass added to the continuous phase from the dispersed second phase. The equation for conservation of momentum is:

$$\frac{\partial}{\partial t}(\rho \vec{v}) + \nabla \cdot (\rho \vec{v}\vec{v}) = -\nabla p + \nabla \cdot (\tau_{eff}) + \rho \vec{g} + \vec{F} \tag{2}$$

where p is the static pressure, τ_{eff} is the stress tensor, and $\rho\vec{g}$ and $\vec{F}$ are the gravitational and external body forces, respectively. The energy equation is:

$$\frac{\partial}{\partial t}(\rho E) + \nabla \cdot (\vec{v}(\rho E + p)) = \nabla \cdot (k_{eff} \nabla T - \sum_j \bar{J}_j + (\bar{\tau}_{eff} \cdot \vec{v})) + S_h \tag{3}$$

where k_{eff} is the effective conductivity, and $\vec{J}_j$ is the diffusion flux of species j. S_h includes the heat of chemical reaction and any other volumetric heat sources. To determine this term, we use the relation:

$$S_h = -\sum_j \frac{h_j^0}{M_j} R_j \tag{4}$$

where h_j^0 is the enthalpy of formation of species j, R_j is the volumetric rate of creation of species j, and M_j is the molar mass of species j.

If it is necessary to consider the equations for the chemical components, we can obtain the concentration of each component Y_i by solving the equation for its convection-diffusion transfer. In general, this equation has the following form:

$$\frac{\partial}{\partial t}\left(\rho Y_j\right) + \nabla\left(\rho \vec{\upsilon} Y_j\right) = -\nabla \cdot \vec{J}_j + R_j + S_j \tag{5}$$

where S_j is the level of additional formation of the *j*-th component from a dispersed phase or other source.

The RNG-based *k*-e turbulence model was used for aerodynamic prediction [32]. The **transport equations** have similar form to that of a standard *k*-e model:

$$\frac{\partial}{\partial t}(\rho k) + \frac{\partial}{\partial x_i}(\rho k u_i) = \frac{\partial}{\partial x_j}\left[\left(\alpha_k \mu_{eff}\right)\frac{\partial k}{\partial x_j}\right] + G_k + G_b - \rho\varepsilon - Y_M, \tag{6}$$

$$\frac{\partial}{\partial t}(\rho \varepsilon) + \frac{\partial}{\partial x_i}(\rho \varepsilon u_i) = \\ = \frac{\partial}{\partial x_j}\left[\left(\alpha_\varepsilon \mu_{eff}\right)\frac{\partial \varepsilon}{\partial x_j}\right] + C_{1\varepsilon}\frac{\varepsilon}{k}(G_k + C_{3\varepsilon}G_b) - C_{2\varepsilon}\rho\frac{\varepsilon^2}{k} - R_\varepsilon \tag{7}$$

In these equations, G_k represents the generation of turbulence kinetic energy due to the mean velocity gradients, G_b is the generation of turbulence kinetic energy due to buoyancy, and Y_M represents the contribution of the fluctuating dilatation in compressible turbulence to the overall dissipation rate. The quantities α_k and α_ε are the inverse effective Prandtl numbers for *k* and e, respectively.

The main difference between the RNG and standard *k*-e models lies in the additional term in the e equation, which is given by

$$R_\varepsilon = \frac{C_\mu \rho \eta^3 (1 - \eta/\eta_0)}{1 + \beta\eta^3}\frac{\varepsilon^2}{k} \tag{8}$$

where C_μ, η_0, β are the empirical constants.

Let us consider the chemical reactions *r*, formed as follows:

$$\sum_{i=1}^{N} \nu'_{i,r} \mathrm{M}_i \underset{k_{b,r}}{\overset{k_{f,r}}{\Leftrightarrow}} \sum_{i=1}^{N} \nu'_{i,r} \mathrm{M}_i \tag{9}$$

where N, is the number of chemical components in the system; $\nu_{i,r}$ is the stoichiometric coefficient for the *i*-th reagent in the reaction *r*; $\nu_{i,r}$ is the stoichiometric coefficient for the *i*-th product of the reaction *r*; M_i is the symbol for the *i*-th chemical component; $k_{f,r}$ is the direct velocity constant for the reaction *r*; and $k_{b,r}$ is the reverse velocity constant for the reaction *r*. The net source of the *i*-th chemical component obtained via the reaction R_i is calculated as the sum of sources N_R of the Arrhenius reactions in which the components take part:

$$R_i = M_{\varpi,i} \sum_{r=1}^{N_R} R_{i,r} \tag{10}$$

where $M_{\varpi,i}$ is the molar mass of the *i*-th component, and $R_{i,r}$ is the Arrhenius velocity of formation/decomposition of the *i*-th component in the reaction *r*.

The velocity constant for the direct reaction *r* is calculated using the Arrhenius expression:

$$k_{f,r} = A_r T^{\beta_r} e^{-E_r / RT} \tag{11}$$

where A_r is a pre-exponential factor; β_r is the temperature exponent; E_r is the activation energy for the reaction; and R is the universal gas constant.

If the reaction is reversible, the reverse velocity constant is defined as follows:

$$k_{b,r} = \frac{k_{f,r}}{K_r} \tag{12}$$

where K_r is the balance constant for the reaction *r*.

The Eddy dissipation concept (EDC) model (based on detailed Arrhenius chemical kinetics incorporated in flames with turbulent fluctuations) has been used for calculation of a gas turbine combustor [30]. The EDC model assumes that the reaction occurs in small turbulent structures called fine scales. Species react in these fine structures over a given timescale governed by Arrhenius rates, and the reactions are integrated numerically using the ISAT algorithm. Thus, to calculate the net source of species *i* via chemical reaction, it is necessary to find the fine scale and time scale. The length fraction and time scales are:

$$\xi^* = \tilde{N}_\xi \left(\frac{\nu \varepsilon}{k} \right)^{3/4}, \quad \tilde{N}_\xi = 2.377 \tag{13}$$

$$\tau^* = \tilde{N}_\tau \left(\frac{\nu}{\varepsilon} \right)^{1/2}, \quad \tilde{N}_\tau = 0.4082 \tag{14}$$

The detailed expanded chemical mechanisms that describe the combustion of hydrocarbon fuel are developed for the combustion of CO/H_2 mixtures. There are also additional simplified or so-called global mechanisms for CFD modeling, which are mainly used for calculations of the oxidation of hydrocarbon fuels and synthesis gases.

In the present work, we use an approved early [36, 37] simplified 35-reaction reducing mechanism (Table 1) to carry out a detailed analysis of the combustion operating processes.

Tab. 1. Reactions in the reducing mechanism

$H+O_2 \rightarrow OH+O$	$OH+O \rightarrow H+O_2$	$O+H_2 \rightarrow OH+H$
$OH+H \rightarrow O+H_2$	$OH+H_2 \rightarrow H_2O+H$	$H_2O+H \rightarrow OH+H_2$
$OH+OH \rightarrow H_2O+O$	$H_2O+O \rightarrow OH+OH$	$H+O_2+M \rightarrow HO_2+M$
$HO_2+H \rightarrow OH+OH$	$HO_2+H \rightarrow H_2+O_2$	$HO_2+OH \rightarrow H_2O+O_2$
$CO+OH \rightarrow CO_2+H$	$CO_2+H \rightarrow CO+OH$	$CH_4(+M) \rightarrow CH_3+H(+M)$
$CH_3+H(+M) \rightarrow CH_4(+M)$	$CH_4+H \rightarrow CH_3+H_2$	$CH_3+H_2 \rightarrow CH_4+H$
$CH_4+OH \rightarrow CH_3+H_2O$	$CH_3+H_2O \rightarrow CH_4+OH$	$CH_3+O \rightarrow CH_2O+H$
$CH_2O+H \rightarrow HCO+H_2$	$CH_2O+OH \rightarrow HCO+H_2O$	$HCO+H \rightarrow CO+H_2$
$HCO+M \rightarrow CO+H+M$	$CH_3+O_2 \rightarrow CH_3O+O$	$CH_3O+H \rightarrow CH_2O+H_2$
$CH_3O+M \rightarrow CH_2O+H+M$	$HO_2+HO_2 \rightarrow H_2O_2+O_2$	$H_2O_2+M \rightarrow OH+OH+M$
$OH+OH+M \rightarrow H_2O_2+M$	$H_2O_2+OH \rightarrow H_2O+HO_2$	$H_2O+HO_2 \rightarrow H_2O_2+OH$
$H+OH+M \rightarrow H_2O+M$		$H+H+M \rightarrow H_2+M$

The validity of using this simplified mechanism in three-dimensional investigations of synthesis gas combustion was demonstrated in [38]. To analyze the possibility of using a low-emission gas turbine combustor (Fig. 4) for low-calorie synthesis gas burning, the corresponding three-dimensional calculations were performed. The synthesis gas supplied to the combustor has the following composition (vol.): water vapor (H_2O) 53.4%; hydrogen (H_2) 34.9%; carbon monoxide (CO) 4.3%; carbon dioxide (CO_2) 6.6%; methane (CH_4) 0.7%; nitrogen (N_2) 1.0%.

Figure 5 shows the aerodynamic structure of the working fluid flow inside the combustor. After the high-pressure compressor, the air entering the chamber diffuser undergoes a complex motion, reversing direction twice. As it moves within the space of the annular combustor, it enters the flame tube through the secondary air and film cooling holes, and then twists, passing through the two radial swirlers of the

first and second channels and the annular mixing chambers in the front burner unit.

The airflow passing through the radial swirlers of the first and second channels deviates from the original direction, and spreads out in the form of circular swirling jets along the lateral surface of the annular mixing chambers in the area of the frontal device. The rotational movement of the air leads to the appearance of centrifugal forces, causing increased pressure at the periphery of the stream (near the walls) and reduced pressure in its axial part. Thus, a circulating backflow occurs in the central part of the frontal device.

This recirculation zone is a powerful combustion stabilizer. Hot combustion products circulate in it and ignite fresh portions of the air-fuel mixture, ensuring low-calorific, stable combustion of the synthesis gas. The contours of the gas temperature inside the combustor are shown in Fig. 6.

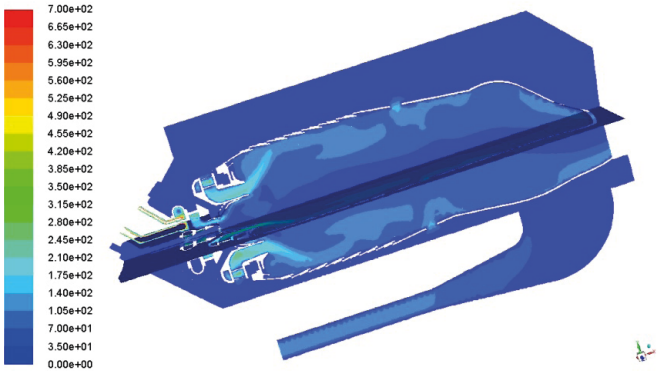

Fig. 5 Distribution of the magnitude of the velocity (m/s) inside the combustor

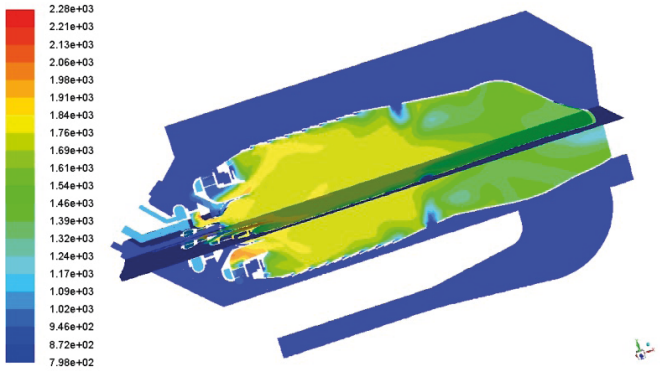

Fig. 6 Contours of the temperature (K) inside the combustor

The maximum temperature zone begins in the central prechamber sections, where despite the significant content of water vapor, the combustion of the synthesis gas is stabilized by the recirculation zone. Note that in some cases, in order to improve the flame stabilization conditions, a method of plasma-chemical combustion intensification [33, 39] may be applied.

The contours of the NO, CO, H_2 and CO_2 mass fractions are shown in Fig. 7. During burning of the synthesis gas at a low average flame temperature, the formation of thermal nitrogen oxides in the combustor volume is significantly suppressed due to the large amounts of steam, and the calculated content of nitrogen oxides in the exit section of the combustor does not exceed 10 ppm. This complies with modern European standards for the emission of toxic components by gas turbine engines.

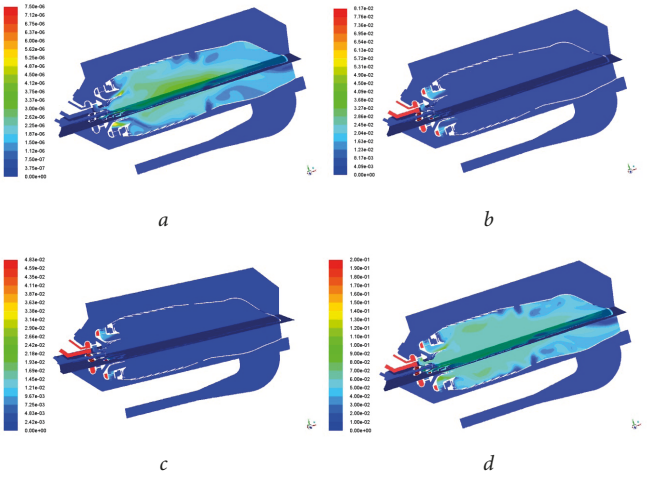

Fig. 7 Contours of the mass fraction of (a) NO; (b) CO; (c) H_2, and (d) CO_2 inside the combustor

Due to the presence of steam, the reactions of complete carbon monoxide CO oxidation are delayed, and the calculated emission of CO at the exit of the combustor is equal to 85 ppm, which also does not exceed the emission standards even for gas turbines that operate on natural gas. The volumetric concentration of CO_2 at the combustor exit is 2.37%, which is lower than the emission of this greenhouse gas by gas turbine engines working on natural gas.

Along with the identified advantages (its high stability of operation on fuels with a high steam content, and low emission of toxic components), the serial combustor considered here needs some structural improvements when operating on synthesis gas, for example: (a) prevention of the possibility of flashback in the region of radial swirlers due to the high temperature of the synthesis gas; (b) changes to the size of the gas supply pipelines due to an increase in the flow rate of synthesis gas compared to natural gas; and (c) development of a more effective means of cooling the flame tube walls, especially in the frontal device area. These will be the subject of further investigation.

CONCLUSION

The use of thermo-chemical heat recovery from the gas turbine energy module of a FPSO makes it possible to obtain synthesis gas with a fairly stable composition, regardless of the methane content of the associated gas used as fuel.

At the maximum permissible mass ratio of steam/gas, i.e. in the range 6–7, the efficiency of the gas turbine energy module of an offshore vessel is about 50%. Three-dimensional calculations of the low-emission gas turbine combustor

demonstrated the possibility of efficient use of associated gas conversion products as the main fuel, and the stability of the burning process. The estimated emissions of the main toxic components (NO_x and CO) are in line with current European emission standards for gas turbine engines.

REFERENCES

1. Organization for Economic Co-operation and Development (2014): *Offshore Vessel, Mobile Offshore Drilling Unit & Floating Production Unit Market Review*. Retrieved from http://www.oecd.org/officialdocuments/publicdisplaydocumentpdf/?cote=c/wp6(2014)13/final&doclanguage=en.

2. Visiongain (2012): *The Mobile Offshore Drilling Units (MODU) Market 2012–2022*. Retrieved from https://www.marketresearch.com/product/sample-6889468.pdf.

3. Stena Drilling (2018): *Stena Drill MAX*. Retrieved from http://stenadrillingmediabank.s3-eu-west-1.amazonaws.com/stena/wp-content/uploads/2018/04/11110204/Stena-DrillMAX_Technical-Specification_APR2018.pdf.

4. Stena Drilling (2018): *Stena Don*. Retrieved from https://www.stena-drilling.com/stena/wp-content/uploads/2017/08/80845_Stena_DON_Brochure_A4_FINAL_LO.pdf.

5. OCYAN (2017): *FPSO Pioneiro de Libra*. Retrieved from http://www.ocyansa.com/en/fleet/fpso-pioneiro-de-libra.

6. Offshore Magazine (2018): *OTC 2018: FPSO Market Recovery Under Way, Says EMA Report*. Retrieved from https://www.offshore-mag.com/production/article/16804111/otc-2018-fpso-market-recovery-under-way-says-ema-report.

7. Offshore Technology (2018): Report: 55 FPSOs to Start Operations by 2022. Retrieved from https://www.offshore-technology.com/news/report-55-fpsos-start-operations-2022/.

8. Offshore Magazine (2002): *Leadon FPSO Delivered on Time, Complete, Within Budget*. Retrieved from https://www.offshore-mag.com/production/article/16759844/leadon-fpso-delivered-on-time-complete-within-budget.

9. ENI (2016): B*lock 15-06 East Hub Development Project*. Retrieved from https://www.eni.com/docs/en_IT/enicom/publications-archive/publications/brochures-booklets/countries/brochure_eni_angola_ese_web.pdf.

10. Aker Floating Production (2009): *FPSO Dhirubhai-1*. Retrieved from http://www.akerfloatingproduction.com/s.cfm/3-12/FPSO-Dhirubhai-1-Operation.

11. OCYAN (2017): *FPSO Pioneiro de Libra*. Retrieved from http://www.ocyansa.com/en/fleet/fpso-pioneiro-de-libra.

12. OCYAN (2017): *FPSO Cidade de Itajaí*. Retrieved from https://api.ocyan-sa.com/sites/default/files/2018-09/cidade_do_itajai_0.pdf.

13. Offshore Technology (2018): *Triton Oil Field, North Sea Central*. Retrieved from https://www.offshore-technology.com/projects/triton/.

14. MAN Diesel & Turbo (2013): *Offshore Power Module*. Retrieved from https://marine.man-es.com/docs/default-source/shopwaredocumentsarchive/offshore-power-module.pdf?sfvrsn=c2dd9a8_4.

15. Caterpillar Global Petroleum (2013): *Offshore Power Generation Module*. Retrieved from https://s7d2.scene7.com/is/content/Caterpillar/C10340375.

16. Siemens (2019): *We Power the World with Innovative Gas Turbines: Siemens Gas Turbine Portfolio*. Retrieved from https://new.siemens.com/global/en/products/energy/power-generation/gas-turbines.html.

17. Olszewski W., Dzida M. (2018): *Selected Combined Power Systems Consisted of Self-Ignition Engine and Steam Turbine*. Polish Maritime Research, No.1, Vol. 25, 198–203.

18. Domachowski Z., Dzida M. (2019): *Applicability of Inlet Air Fogging to Marine Gas Turbine*. Polish Maritime Research, Vol. 26, No.1, 15-19.

19. Mazzetti M.J., Nekså P., Walnum H.T., Hemmingsen A.K. (2014): *Energy-Efficient Technologies for Reduction of Offshore CO_2 Emissions*. Oil and Gas Facilities, Vol. 3, No. 1, 8996.

20. Tarelko W. (2018): *Application of Redundancy in Ship Power Plants of Offshore Vessels*. New Trends in Production Engineering, Vol. 1, No. 1, 443-452.

21. Tarelko W. (2018): *Redundancy as a Way Increasing Reliability of Ship Power Plants*. New Trends in Production Engineering. Vol. 1, No. 1, 515-522.

22. The UK Oil and Gas Industry Association Ltd. (2015): *Offshore Gas Turbines and Dry Low NOx Burners. An Analysis of the Performance Improvement*. Retrieved from https://oilandgasuk.co.uk/wp-content/uploads/2015/05/producys-cayrgory.pdf.

23. Cherednichenko O., Serbin S. (2018): *Analysis of Efficiency of the Ship Propulsion System with Thermochemical Recuperation of Waste Heat*. Journal of Marine Science and Application, Vol. 17, No.1, 122-130.

24. Cherednichenko O. (2015): *Analysis of Efficiency of Diesel-Gas Turbine Power Plant with Thermo-Chemical Heat Recovery.* MOTROL: Commission of Motorization and Energetics in Agriculture. Vol.17, No. 2, 25-28.

25. Cherednichenko O. (2019): *Efficiency Analysis of Methanol Usage for Marine Turbine Power Plant Operation Based on Waste Heat Chemical Regeneration.* Problemele Energeticii Regionale, No.1, 102-111.

26. Cherednichenko O., Serbin S., Dzida M. (2019): *Application of Thermo-Chemical Technologies for Conversion of Associated Gas in Diesel-Gas Turbine Installations for Oil and Gas Floating Units.* Polish Maritime Research, 3(103), Vol. 26, 181187.

27. Dzida M., Girtler J. (2016). *Operation Evaluation Method for Marine Turbine Combustion Engines in Terms of Energetics.* Polish Maritime Research, 4(92), Vol. 23, 6772.

28. Farry M. (1998): *Ethane from Associated Gas Still the Most Economical*. Retrieved from https://www.ogj.com/articles/print/volume-96/issue-23/in-this-issue/gas-processing/ethane-from-associated-gas-still-the-most-economical.html.

29. Budanova N.A., Vantsovskiy V.G., Korotich E.V. (2004): *Development of the Low-Emission Combustion Chambers for the Gas Turbine Engines DN70, DN80, DB90*. Marine and Energetic Gas Turbine Building, Vol. 1, GTR&PC "Zorya-Mashproekt", Nikolaev, 31-35.

30. Serbin S. I., Matveev I. B., Mostipanenko G. B. (2011): *Investigations of the Working Process in a "Lean-Burn" Gas Turbine Combustor With Plasma Assistance*. IEEE Transactions on Plasma Science, Vol. 39, No. 12, 3331-3335.

31. Launder B.E., Spalding D.B. (1972): *Lectures in Mathematical Models of Turbulence.* Academic Press, London.

32. Choudhury D. (1993): *Introduction to the Renormalization Group Method and Turbulence Modeling.* Fluent Inc. Technical Memorandum TM-107, 1993.

33. Serbin S.I. (1998): *Modeling and Experimental Study of Operation Process in a Gas Turbine Combustor with a Plasma-Chemical Element*. Combustion Science and Technology, Vol. 139, 137-158.

34. Serbin S.I. (2006): *Features of Liquid-Fuel Plasma-Chemical Gasification for Diesel Engines*. IEEE Transactions on Plasma Science, Vol. 34, No. 6, 2488-2496.

35. Matveev I., Serbin S., Mostipanenko A. (2007): *Numerical Optimization of the „Tornado" Combustor Aerodynamic Parameters.* Collection of Technical Papers - 45th AIAA Aerospace Sciences Meeting, Reno, Nevada, AIAA 2007-391, Vol. 7, 4744-4755.

36. Serbin S., Goncharova N. (2017): *Investigations of a Gas Turbine Low-Emission Combustor Operating on the Synthesis Gas*. International Journal of Chemical Engineering, Vol. 4, 1-14.

37. Serbin S.I., Matveev I.B., Goncharova N.A. (2014): *Plasma Assisted Reforming of Natural Gas for GTL. Part I*. IEEE Transactions on Plasma Science, Vol. 42, No. 12, 3896-3900.

38. Matveev I.B., Serbin S.I., Vilkul V.V., Goncharova N.A. (2015): *Synthesis Gas Afterburner Based on an Injector Type Plasma-Assisted Combustion System*. IEEE Transactions on Plasma Science, Vol. 43, No. 12, 3974-3978.

39. Gatsenko N.A., Serbin S.I. (1995): *Arc Plasmatrons for Burning Fuel in Industrial Installations*. Glass and Ceramics, Vol. 51(11-12), 383-386.

CONTACT WITH THE AUTHORS

Oleksandr Cherednichenko
e-mail: cherednichenko.aleksandr65@gmail.com
Admiral Makarov National University of Shipbuilding,
Heroyiv Ukraine av. 9, 54025 Mykolaiv
Ukraine

Serhiy Serbin
e-mail: serbin1958@gmail.com
Admiral Makarov National University of Shipbuilding,
Heroyiv Ukraine av. 9, 54025 Mykolaiv
Ukraine

Marek Dzida
e-mail: dzida@pg.edu.pl
Gdańsk University of Technology,
11/12 Gabriela Narutowicza Street, 80-233 Gdańsk
Poland